Published in final edited form as:
Neurobiol Aging. 2012 August ; 33(8): 1699–1715. doi:10.1016/j.neurobiolaging.2011.06.001.

Testing the white matter retrogenesis hypothesis of cognitive aging

Adam M. Brickman[a,b,*], **Irene B. Meier**[a], **Mayuresh S. Korgaonkar**[c], **Frank A. Provenzano**[a], **Stuart M. Grieve**[c], **Karen L. Siedlecki**[d], **Ben T. Wasserman**[a], **Leanne M. Williams**[c,e], and **Molly E. Zimmerman**[f]

[a] Taub Institute for Research on Alzheimer's Disease and the Aging Brain, College of Physicians and Surgeons, Columbia University, New York, NY USA

[b] Gertrude H. Sergievsky Center and Department of Neurology, College of Physicians and Surgeons, Columbia University, New York, NY USA

[c] Brain Dynamics Centre, University of Sydney Medical School and Westmead Millennium Institute, Sydney, Australia

[d] Department of Psychology, Fordham University, New York, NY USA

[e] BRAINnet Foundation, San Francisco, CA USA

[f] Department of Neurology, Albert Einstein College of Medicine, Bronx, NY USA

Abstract

Background—The retrogenesis hypothesis postulates that late-myelinated white matter fibers are most vulnerable to age- and disease-related degeneration, which in turn mediate cognitive decline. While recent evidence supports this hypothesis in the context of Alzheimer's disease, it has not been tested systematically in normal cognitive aging.

Methods—In the current study, we examined the retrogenesis hypothesis in a group (n=282) of cognitively normal individuals ranging in age from 7 to 87 years from the Brain Resource International Database. Participants were evaluated with a comprehensive neuropsychological battery and were imaged with diffusion tensor imaging. Fractional anisotropy (FA), radial diffusivity (RD), and axial diffusivity (DA), measures of white matter coherence, were computed in two prototypical early-myelinated fiber tracts (posterior limb of the internal capsule, cerebral peduncles) and two prototypical late-myelinated fiber tracts (superior longitudinal fasciculus, inferior longitudinal fasciculus) chosen to parallel previous studies; mean summary values were also computed for other early- and late-myelinated fiber tracts. We examined age-associated differences in FA, RD, and DA in the developmental trajectory (ages 7 to 30 years) and

*Corresponding author: Taub Institute for Research on Alzheimer's Disease and the Aging Brain, Department of Neurology, College of Physicians and Surgeons, Columbia University, 630 West 168th Street, P&S Box 16, New York, NY 10032, tel: 212 342 1348, fax: 212 342, 1838, amb2139@columbia.edu.

Disclosure statement

Dr. Grieve has received consulting fees from brain Resource Ltd. Dr. Williams has received consulting fees and stock options in Brain Resource Ltd, and is a stock holder in Brain Resrouce Ltd. She has received advisory board fees from Pfizer. Other authors report no actual or potential conflicts of interest.

degenerative trajectory (ages 31 to 87 years), and tested whether the measures of white matter coherence mediated age-related cognitive decline in the older group.

Results—FA and DA values were greater for early-myelinated fibers than for late-myelinated fibers, and RD values were lower for early-myelinated than late-myelinated fibers. There were age-associated differences in FA, RD, and DA across early- and late-myelinated fiber tracts in the younger group, but the magnitude of differences did not vary as a function of early or late myelinating status. FA and RD in most fiber tracts showed reliable age-associated differences in the older age group, but the magnitudes were greatest for the late-myelinated tract summary measure, inferior longitudinal fasciculus (late fiber tract), and cerebral peduncles (early fiber tract). Finally, FA in the inferior longitudinal fasciculus and cerebral peduncles and RD in the cerebral peduncles mediated age-associated differences in an executive functioning factor.

Discussion—Taken together, the findings highlight the importance of white matter coherence in cognitive aging and provide some, but not complete, support for the white matter retrogenesis hypothesis in normal cognitive aging.

Keywords

MRI; diffusion tensor imaging; aging; cognition; retrogenesis; BRAINnet

1. Introduction

The retrogenesis hypothesis of cognitive aging postulates that breakdown of late-myelinated white matter fibers mediates age-associated cognitive decline. The theory stems from the observation that during early life maturation, white matter fiber tracts develop at variable rates, with some fully developed by birth and early childhood and others continuing development through adolescence and early adulthood (Homae et al., 2010; Huppi et al., 1998; Huttenlocher and Dabholkar, 1997; Kinney et al., 1988; Rakic et al., 1986; Takeda et al., 1997). Fibers that myelinate early during brain development are thought to be more robust than later-myelinated fibers and thus, in the context of degeneration due to brain disease or normal aging-related processes, might be less susceptible to damage (Stricker et al., 2009). Given consistent observations of the importance of white matter in normal and abnormal cognitive development and aging (Brickman et al., 2009; Brickman et al., 2006; Chanraud et al., 2010; Fellgiebel et al., 2008; Grieve et al., 2007; Huppi, 2010; Sullivan and Pfefferbaum, 2006), identification of the factors that increase susceptibility to white matter degeneration remains an important avenue of research.

In the context of aging, the retrogenesis hypothesis has been applied primarily to the study of Alzheimer's disease (AD) (Reisberg et al., 1999). For example, Bartzokis (Bartzokis, 2009; Bartzokis et al., 2007) codified the hypothesis by proposing that the late-myelinated small-diameter cortico-cortical axons are the earliest and most affected in AD and that damage to these fibers increases susceptibility to β-amyloid deposition, whereas heavily myelinated brain regions are less likely to develop AD pathology (Braak et al., 2000). This damage to the white matter microstructure, in turn, causes a reduction in neural information transmission across the cortical regions that mediate higher cognitive function, resulting in the neuropsychological syndrome that defines the disease. Thus, it is both the susceptibility to AD-related pathology in late-developing neurons and the disturbance in neural transmission that may cause the cognitive impairment seen in AD. In theory, however, the retrogenesis hypothesis may similarly account for age-associated cognitive decline observed in the absence of AD or other frank neurodegenerative pathology. Late-myelinated fibers may be more vulnerable to age-associated lipid oxidation, and increases in toxicity due to iron release may additionally damage white matter (Hemdan and Almazan, 2006) irrespective of pathological features associated with AD. In the current study, we sought to

determine whether similar principles may help explain the pattern of white matter degeneration and cognitive decline in healthy subjects as well.

Remarkable advancements in acquisition and analysis of neuroimaging data over the past twenty years have revolutionized our ability to visualize, quantify, and make inferences about the neurobiological underpinnings of cognitive development and aging. Among the most significant developments is the implementation of diffusion tensor imaging (DTI), which is a technique with the ability to estimate the orientation and coherence of white matter fiber tracts through the quantification of diffusion properties of water. Diffusion tensor imaging exploits the propensity of water molecules to perfuse parallel to the white matter fibers because of the physical constraint created by the lipid myelin sheath (Le Bihan et al., 2001; Westlye et al., 2010).

There are several metrics that can be derived from DTI data. *Fractional anisotropy* (FA), a common metric applied to DTI data, refers to the degree to which water molecules diffuse in one direction (i.e., along the fiber axis created by the fiber tract), and is particularly sensitive to the coherence of white matter fiber tracts (Barkovich, 2000; Bartzokis et al., 2003; Basser and Jones, 2002; Song et al., 2002). Highly myelinated white matter bundles organized in similar orientations will have greater FA than fibers that are less myelinated or less organized (Pierpaoli and Basser, 1996; Sullivan et al.). *Axial diffusivity* (DA) is a measure of water diffusion along the primary axis (λ_1) and *radial diffusivity* (RD) refers to the average of the two eigenvalues orthogonal to the primary axis (λ_2, λ_3; see Methods for details). It is important to note that the measure of FA comprises information from DA and RD, providing a metric that reflects the degree to which water diffuses along the principal axis relative to diffusion in the minor axes. Thus, relative differences in DA and RD could be reflected in FA (e.g., an increase in DA coupled with decreased in RD would result in increased FA). Results from animal studies suggest that RD increases with damage to myelin, whereas axonal damage is associated with changes in DA (Song et al., 2003; Song et al., 2002; Song et al., 2005; Sun et al., 2006; Sun et al., 2007). Thus, it is possible that RD is a specific marker of myelin integrity and DA is a specific marker of axonal integrity, although, to our knowledge, these possibilities reflect preliminary observations that have only been made in murine models. Given its exquisite sensitivity to white matter integrity, DTI-derived measures may be particularly useful in examining whether the white matter retrogenesis hypothesis is operative in clinical and non-pathological populations.

Indeed, a recent study by Stricker and colleagues (Stricker et al., 2009) used DTI to examine the retrogenesis hypothesis among patients with AD. They found a disproportionate decrease in FA and increase in RD relative to neurologically-healthy controls in late-myelinated association fiber tracts, particularly in the inferior longitudinal fasciculus, providing evidence in support of retrogenesis. That report may be among the first to compare explicitly the coherence of white matter fiber tracts defined *a priori* as early- *versus* late-myelinated regions in AD and does provide some initial support for the overall theory as applied to AD. Although the retrogenesis hypothesis has been proposed as a putative explanation for both normal age-related and pathology-related cognitive dysfunction, to our knowledge it has been tested only in the context of AD. Nonetheless, several investigators have more generally examined the pattern of white matter changes with age and have revealed a pattern of anterior-to-posterior diminution of FA and increase in diffusivity with increasing age, which corresponds to the degree of observed age-associated cognitive change (Ardekani et al., 2007; Bucur et al., 2008; Damoiseaux et al., 2009; Grieve et al., 2007; Head et al., 2004; Madden et al., 2004; McLaughlin et al., 2007; O'Sullivan et al., 2001; Sullivan et al., 2006). These observations may reflect a retrogenesis pattern, as anterior regions comprise more late-myelinated fibers than posterior regions.

In the current study, we sought to examine explicitly the white matter retrogenesis hypothesis in normal aging. Diffusion tensor MR imaging and comprehensive neuropsychological testing were obtained on neurologically, psychiatrically, and medically healthy individuals ranging in age from 7- to 87-years. Regions-of-interest were chosen *a priori* to represent prototypical early-myelinated and late-myelinated fibers, based on previous literature (Stricker et al., 2009). The retrogenesis hypothesis would generate several predictions. First, because early-myelinated fibers develop almost to maturity pre- and perinatally (Huang, 2010; Huang et al., 2009; Huang et al., 2006; Yakovlev and Lecours, 1967) and tend to be more robust (Choi et al., 2005; Stricker et al., 2009), we expected greater overall white matter integrity in early-myelinated fiber tracts compared with late-myelinated fiber tracts and age-associated increases in white matter integrity from early childhood to early adulthood (i.e., during brain maturation/development) to be more pronounced for later-myelinated fibers. Second, we expected greater age-related decreases in later-myelinated fiber tracts among adults, reflecting their relative vulnerability to age-related breakdown. Finally, we predicted that age-related white matter integrity in late-myelinated fibers would be more predictive of cognitive functioning among older adults than white matter integrity in early-myelinated fibers and would mediate the relationship between age and cognition.

2. Methods

2.1. Subjects

Diffusion tensor MRI and neuropsychological evaluations were conducted in 282 healthy individuals (age range 7- to 87-years-old) from the Brain Resource International Database, accessed via the independent BRAINnet Foundation (www.BRAINnet.net). The database comprises data collected from six primary sites throughout the world (Gordon et al., 2005). For the current study, only participants from one site in Australia (Flinders University) were included, as this was the only site to collect DTI data. Participants were assessed with the Somatic and Psychological Health Report (SPHERE) (Hickie et al., 2001) and excluded if they had a psychiatric history. Other exclusionary criteria included histories of brain injury, neurological illness, significant medical condition and/or drug or alcohol addiction. Individuals with first degree family members with attention deficit hyperactivity disorder, schizophrenia, bipolar disorder, or genetic disorder were also excluded. The research was approved by local ethics committees and informed consent was obtained on all participants or their surrogates after assent was established (in the case of minors).

Table 1 displays demographic characteristics for the entire sample and for the sample divided into two groups, based on a threshold age of 30 years. This age threshold was determined following visual inspection of the DTI data plotted as a function of age (see below). The average point of inflection, consistent with other lifespan reports (Kochunov et al., 2010), was at about age 30. By design, the two groups differed significantly in age ($t(280)=37.86$, $p<0.001$). The older group also had significantly more years of education ($t(275)=6.77$, $p<0.001$) reflecting the fact that a substantial proportion of the younger group had not yet completed school. However, the two groups were similar in sex distribution ($\chi^2(1)=0.11$, $p=0.738$).

2.2. MRI scan acquisition

Magnetic resonance imaging was conducted on a 1.5 T Siemens Sonata (Erlangen, Germany) system. The MRI protocol comprised a 3D T1-weighted image (TR = 9.7 ms; TE = 4 ms; Echo train: 7; Flip Angle = 12°; TI = 200 ms; NEX = 1) and a proton-density/T2-weighted dual echo sequence (TR: 7530 ms; TE: 15/105 ms; Echo train: 7; Flip Angle: 180°; NEX: 1). Diffusion tensor imaging was acquired with a DTI echo planar imaging

sequence (TR: 160 ms; TE: 88 ms; Fat Saturation; NEX: 4; FOV: 22cm X 22cm), which included a baseline image (b=0) and 12 diffusion orientations with b-values of 1250. For DTI, there were 32, 6.5 mm contiguous slices obtained with an in- plane matrix of 128 × 128 and a resolution of 1.72mm^2.

2.3. Diffusion tensor imaging analysis

Diffusion tensor imaging data were preprocessed and analyzed with the fMRIB Diffusion Toolbox (FDT) and tract based spatial statistics (TBSS) of the fMRI Software Library (FSL 4.1.3. release; www.fmrib.ox.ac.uk/fsl) (Smith et al., 2006; Smith et al., 2004). First, raw DTI data for each subject were corrected for head movement and eddy current distortions with an affine registration to the T2-weighted non-diffusion (b=0) image. A binary brain mask was generated from the b=0 image. Diffusion tensor models were then fitted independently for each voxel within the brain mask and the lengths of the longest (λ_1), middle (λ_2) and shortest (λ_3) axes defining the diffusion tensor for the voxel were estimated. Voxel wise fractional anisotropy (FA) calculations were performed to generate an FA image. Fractional anisotropy was defined as: $(3/2)^{1/2} \times [((\lambda_1 - \lambda_{av})^2 + (\lambda_2 - \lambda_{av})^2 + (\lambda_3 - \lambda_{av})^2) / (\lambda_1 + \lambda_2 + \lambda_3)]^{1/2}$, where λ_n = the eigenvalues describing the diffusion tensor, and λ_{av} is the mean diffusivity $((\lambda_1 + \lambda_2 + \lambda_3)/3)$. Images of the first ($\lambda_1$), second ($\lambda_2$) and third eigenvalues (λ_3) were also generated for each participant, which were used to derive RD (i.e., mean of λ_2 and λ_3) and DA (i.e, λ_1) values.

2.3.1. Extraction of FA, DA, and RD values for major WM tracts for each subject—

Fractional anisotropy images generated for each participant were first aligned to the FMRIB58_FA template and affine transformed into MNI152 1mm^3 standard space atlas using the nonlinear registration tool FNIRT (Andersson et al., 2007a; Andersson et al., 2007b). An average FA image was then generated and thinned to create a white matter skeleton representing the centers of all white matter tracts common to all subjects. A recent report by Westyle and colleagues (Westlye et al., 2010) checked explicitly the warping of brains across the entire age span to a standard template and concluded that robust native to standard warping is achieved across a wide age group (8–80 years). A threshold of FA ≥ 0.2 was applied to include the major white matter pathways while avoiding peripheral tracts that are more vulnerable to intersubject variability and/or partial volume effects with grey matter. Each subject's aligned FA image was then projected onto the mean FA skeleton by assigning each skeleton voxel by the maximum FA value found in a direction perpendicular to the tract. This approach results in a standard space FA skeleton of the major WM tracts for each subject accounting for any residual registration misalignments and variability in exact tract location between subjects (Smith et al., 2006). The non-FA images (λ_1, λ_2 and λ_3) were also projected onto the skeleton using the same non-linear warping parameters and skeleton projection vectors calculated for the FA images.

Next, we used the JHU ICBM-DTI-81 white matter labels and white matter tractography atlases (Hua et al., 2008; Mori et al., 2008) to label sections of the WM skeleton corresponding to the following major WM tracts in both brain hemispheres: 1. Tracts in the brain stem – corticospinal tract, medial lemniscus, inferior-middle-superior cerebellar peduncle, pontine fiber tracts; 2. Projection fibers–anterior-superior-posterior corona radiata, anterior and posterior limb of internal capsule, retrolenticular part of the internal capsule, cerebral peduncle, posterior thalamic radiation; 3. Association fibers - superior longitudinal fasciculus, superior fronto-occipital fasciculus, inferior longitudinal fasciculus, uncinate fasciculus, sagittal stratum, external capsule, cingulum (cingulate gyrus and hippocampal sections), fornix and stria terminalis; 4. Commissural fibers genu, body and splenium of corpus callosum. Average FA values for each WM tract were calculated from the WM skeleton. The binary mask of each label was used to calculate the average *FA,* λ_1, λ_2 and λ_3

values for each WM tract from the WM skeleton. λ_1 values were used to represent DA, and the average of the λ_2 and λ_3 values were used to represent RD.

2.3.2. Selection of regions-of-interest—Two regions-of-interest (ROI) representing prototypical early and late myelinated fiber tracts, respectively, were selected based on the recent report of Stricker and colleagues (Stricker et al., 2009) and from Makris and colleagues (Makris et al., 2007). For early-myelinated fibers, we selected the posterior limb of the internal capsule (PLIC) and the cerebral peduncles (CP). For late-myelinated fiber tracts, we selected the superior longitudinal fasciculus (SLF) and the inferior longitudinal fasciculus (ILF). These ROIs were chosen based on a rich neuropathological literature that has described the developmental trajectory of white matter fibers (Brody et al., 1987; Kinney et al., 1988; Yakovlev and Lecours, 1967), desire to limit late-myelinated ROIs to cortico-cortical projection fibers, and desire to exclude regions that might be affected by Alzheimer's disease (e.g., cingulum bundle) or Wallerian degeneration (Stricker, 2010, personal communication). Mean FA, RD, and DA values from each hemisphere were averaged to generate a single mean value for each ROI. Figure 1 displays the anatomical distribution of the primary ROIs.

Recognizing that selection of only two ROIs to represent early- and late-myelinated fibers does not take full advantage of the rich neuroimaging data generated, we calculated two additional "early" and "late" summary scores, which excluded the primary ROIs. To do this, we selected fiber tracts that could be characterized unambiguously (Braak and Braak, 1996; Burgel et al., 2006; Stricker et al., 2009; Yakovlev and Lecours, 1967) as early- or late-myelinated and took the overall mean FA, RD, and DA values of all the tracts included after averaging left and right hemispheres (where applicable). Early fibers included the following tracts: inferior cerebellar peduncles, superior cerebellar peduncle, anterior limb of the internal capsule, retrolenticular part of the internal capsule, and superior fronto-occipital fasciculus. Late-myelinated fibers included: genu of the corpus callosum, body of the corpus callosum, splenium of the corpus callosum, fornix, and uncinate fasciculus. These summary ROIs were used to examine age and cognitive effects (see below).

2.4. Neuropsychological assessment

Participants were evaluated with IntegNeuro™, a standardized computerized neuropsychological battery that has been shown to be valid and reliable ((Clark et al., 2006; Gunstad et al., 2006; Paul et al., 2005; Williams et al., 2010; Williams et al., 2005) see (Brain Resource, 2010) for complete description of battery and detailed summary of psychometric properties)). Briefly, the battery was presented with a touch-screen computer (NEC MultiSync LCD 1530V), task instructions were presented on the computer screen or via headphones, and responses were recorded by the touch screen or, for verbal responses, recorded and scored later. The following tasks were included in the current analyses. The battery was utilized because it is part of the standard assessment given to all participants in the Brain Resource International Database.

2.4.1 Learning and memory—Verbal Memory Recall was evaluated with a verbal list learning task on which participants were read a list of 12 words over 4 learning trials. Following the 4 learning trials, there was a distracter trial that participants were asked to recall after presentation. Immediately following the distracter trial, participants were asked to free recall the initial 12 words. A long delay free recall trial was completed following a 20-minute interval, followed by a recognition trial. Variables used in the current study included total learning score across the 4 learning trials, total short delay free recall score, and total long delay free recall score.

A computerized adaptation of the Austin Maze task (Milner, 1965; Walsh, 1985) required participants to identify a hidden path from the beginning point at the bottom to the endpoint at the top of an 8 × 8 matrix of circles. Each navigated move was given feedback regarding whether or not it was correct and a total of 24 consecutive correct moves was required to complete the maze successfully. Only one maze was presented across trials; the task was discontinued when the participant either completed the maze twice without error or after 10min. The dependent measure was the total maze time.

2.4.2. Language—Word Generation was evaluated with a letter and category fluency task. For letter fluency, participants named as many words possible within three separate 60s trials, each beginning with a different letter of the alphabet (F, A, and S). For category fluency participants were asked to name as many animals as quickly as possible in a 60s trial. Dependent measures used included total scores of each task.

2.4.3 Sensori-motor function—A simple Motor Tapping task was used in which participants tapped a circle on the touch-screen with their index finger as quickly as possible for a single 60s trial. The total number of taps with the dominant hand was the dependent variable.

A Choice Reaction Time task was implemented in which participants attended to the computer screen as one of four target circles was illuminated in pseudo-random sequence over a series of trials. For each trial, the participant was required to touch the illuminated circle as quickly as possible following presentation. The interval between the 20 trials varied between 2–4s randomly. The dependent measure was the mean reaction time across trials.

2.4.4. Attention—Span of Visual Memory was evaluated with a task based on the Spatial Span test from the Wechsler Memory Scale III (Wechsler, 1999); it is a visual analogue of the digit span test. An array of squares distributed randomly about the computer screen was highlighted in sequential order on each trial. Participants were asked to repeat the order in which the squares were highlighted by touching the squares with their index finger. The task was administered in both forward and reverse directions. Total score was the dependent variable.

For Digit Span forward and Digit Span backward tasks, participants were presented a series of digits one-by-one and then asked to type in the digits on a numeric keypad in forward or reverse order, respectively. The number of digits in each sequence was gradually increased from 3 to 9, with two trials for each level. The dependent variable was the maximum number of digits reproduced without error.

A two-part Switching of Attention task based on the Trailmaking Test (Reitan, 1958) was administered. For Part 1, participants were presented with 25 encircled numbers spread randomly about the computer screen and asked to connect the number in sequential order as quickly as possible.

2.4.5. Executive functioning—Part 2 of the Switching of Attention task was used as a measure of executive functioning. For this task, participants were required to connect 25 sequential and alternating numbers and letters as quickly as possible. Time to completion was the dependent variable for each part.

2.5. Statistical analysis

Hypotheses were addressed in two stages. First, we compared mean FA, RD, and DA values across the primary early- and late-myelinated fibers with general linear models in which

region was a within-subjects factor and age and sex were covariates. Next, we sought to examine the association between age and FA in early- and late-myelinated fibers during the developmental trajectory (Younger Group) and during the degenerative trajectory (Older Group). Separate multiple regression analyses controlling for sex were constructed that examined the association of age with FA, RD, and DA in early- and late-myelinated fiber tracts, stratified by Age Group, and standardized β weights were compared. As standardized β weights are expressed in standard deviation units, differences among β values reflect differences in effect size. The age cutoff for the Younger Group and Older Group stemmed from inspection of scatterplots comparing age with the DTI metrics, which revealed patterns that were consistent with other lifespan DTI data (Kochunov et al., 2010). Finally, in the Older Group only, we examined the association of FA, RD, and DA in early- and late-myelinated fibers with neuropsychological test performance with multiple regression analysis, controlling for age, sex, and education.

For neuropsychological data reduction and to define latent cognitive domains represented by the covariation of neuropsychological test performance, we subjected performance measures on the neuropsychological battery to an exploratory factor analysis. We used direct oblimin non-orthogonal matrix rotation, with the assumption that different cognitive domains are not truly independent (orthogonal) from each other. Factors were extracted based on eigenvalues of greater than 1.0 and regression based factor scores were derived and used as cognitive outcome measurements. We determined which factors showed significant age effects and tested whether FA, RD, and DA in early- and late-myelinated fibers mediate associations between age and neuropsychological test performance with the Sobel test (Baron and Kenny, 1986; Sobel, 1982).

3. Results

Mean FA values varied reliably across the four fiber tracts (main effect of Fiber Tract, $F(3,837)=3990.26$, $p<0.001$). The PLIC had the greatest mean FA values, followed by CP, SLF, and ILF (all pairwise comparisons, $p<0.001$); tract differences between early- and late-myelinated fibers were greater than tract differences within early and late myelinating fibers. A similar pattern was seen for RD (main effect of Fiber Tract, $F(3,837)=2156.96$, $p<0.001$); PLIC had the lowest RD value, followed by CP, SLF, and ILF (all pairwise comparisons, $p<0.001$). A slightly different pattern emerged for DA values. A significant main effect of Fiber Tract ($F(3,837)=2503.58$, $p<0.001$) indicated that mean DA values in the CP were greatest, followed by PLIC, then ILF, and SLF (all pairwise comparisons, $p<0.001$); however, much like with FA, there is a clear difference between the early and late myelinated fibers for DA. Figure 2 displays adjusted FA, RD, and DA mean values across fiber tracts.

Table 2 displays the results from the first series of multiple regression analyses. Age was significantly associated with FA in the primary ROI early- and late-myelinated fibers in both age groups in the expected directions (i.e., positively among younger participants and negatively in older participants). Comparing standardized β weights across fiber tracts and age groups, age appeared to be most greatly related to FA values in the CP (early-myelinated fibers) and ILF (late-myelinated fibers) in both age groups, though effect size differences among ROIs were generally small in the younger age group and greater in the older age group. Examination of the early- and late-myelinated fiber summary variables shows a similar pattern within the Younger Group: increasing FA in early- and late-myelinated fibers was associated with increasing age at similar magnitudes. Among the Older Group, however, there was a clear dissociation between early- and late-myelinated fibers. The slope of age-related FA decline was much greater for late myelinated fibers than for early-myelinated fibers. As the standardized β weights reflect the age-associated

differences in the DTI metrics expressed in standard deviation units, the difference between these two slopes reflects a moderate effect size.

Findings regarding RD paralleled those observed for FA. First, the relationships between age and RD were in the expected directions: negative in the younger group and positive in the older group. Second, RD in CP and ILF was most strongly related to age in both age groups. Third, among the younger group RD for the early fiber summary measure was more strongly related to age than RD for the late fiber summary score, whereas in the older group RD for the summary of late-myelinated fibers was more strongly related to age than RD in the early-myelinated fibers. A somewhat less consistent pattern of results emerged from analysis of DA data. Most measures were not reliably associated with age in either age group (see Table 2). However, like with RD, mean DA for the early fiber summary variable appeared to be more reliably associated with age than DA in late fiber summary variable in the younger group, whereas DA for the late fiber summary measure was more reliably associated with age than the early fiber summary measure in the older group. Figure 3 displays scatterplots of the association between age and FA, RD, and DA measures in the primary ROIs and summary scores across the lifespan.

Factor loadings for neuropsychological test scores derived within the Older Group are displayed in Table 3. Four factors were derived reliably. The first represents variables hypothesized to represent executive abilities, the second comprises performance on tests of memory, the third includes speeded tasks with an attention demand, and the final factor includes language tasks. Controlling for education and sex, age was negatively associated with executive abilities (standardized $\beta=-0.695$, $p<0.001$; overall model $F(3,26)=6.788$, $p=0.002$). Education (standardized $\beta=-0.370$, $p=0.030$) but not sex (standardized $\beta=-0.174$, $p=0.299$) was also associated with executive abilities. Age was not reliably associated with the other two neuropsychological factors (all model F's < 1.80, all p's ≥ 0.190).

Next we entered mean FA, RD, and DA values from early- and late-myelinated fibers into the regression model that examined the association between age and executive functioning. Increased FA in CP (early-myelinated) and in ILF (late-myelinated) fiber tracts was associated with better executive functioning (see Table 4). Fractional anisotropy in the other two primary ROIs or in the early and late summary regions was not related to executive functioning. The Sobel test (Baron and Kenny, 1986; Sobel, 1982) was used to determine whether FA in CP or in ILF significantly mediates the association between age and executive functioning. Indeed, FA in CP (Sobel test statistic=−2.08, p=0.0068) and in ILF (Sobel test statistic = −2.502, p=0.0123) significantly mediated the relationship between age and executive functioning. Lower RD in CP was associated with better executive functioning and RD values in CP mediated the association between age and executive functioning (Sobel test statistic = −2.080, p=0.0375). Axial diffusivity values were not related to executive functioning (see Table 4).

4. Discussion

We examined the white matter retrogenesis hypothesis of cognitive aging by characterizing developmental and degenerative age-related differences in early- and late-myelinated fibers. Using DTI to compute FA, RD, and DA in prototypical early- and late-myelinated fiber tracts (Stricker et al., 2009), we found that early-myelinated tracts have greater FA and DA and lower RD than later-myelinated tracts. These observations suggest that DTI-derived indices, such as FA, RD, and DA, are reasonable proxies for degree of myelination, as earlier-myelinated fibers tend to be more robust than later-myelinated fibers (Choi et al., 2005). In terms of age-related differences, there was relative parity among fiber tracts from early childhood to early adulthood, but with age-associated degeneration the ILF (late-

myelinated) and CP (early-myelinated) fiber tracts showed the greatest effects particularly for FA and RD. As the FA metric is a summary of the three eigenvalues that comprise the diffusion tensor image and, Examination of the early and late fiber summary measures among the older participants showed a very clear dissociation in age-related differences, with later-myelinated fibers showing the greatest age-associated differences among within the older group. Finally, among the older age group, FA in the ILF and CP and RD in the CP appeared to mediate the association between age and decline in executive abilities. Taken together, these findings highlight the importance of white matter coherence in cognitive aging and provide some, but not complete, support for the retrogenesis hypothesis.

In terms of the developmental trajectories examined, we predicted that earlier-myelinated fiber tracts would show a less steep association with increased age than later-myelinated tracts, as histological studies would suggest that tract development in these regions are mostly complete during prenatal and perinatal periods (Dubois et al., 2006; Huppi et al., 1998; Yakovlev and Lecours, 1967). These predictions were generated from neuropathological studies in humans and non-human primates (Brody et al., 1987; Kinney et al., 1988; Yakovlev and Lecours, 1967), which, while able to measure myelin directly, are inherently limited by cause-of-mortality factors and small sample sizes. Our data, like other studies that have examined DTI across the lifespan (Kochunov et al., 2010), suggest that white matter fiber tracts continue to develop until about age 30, at which time they enjoy a brief “plateau” period only to begin degenerating soon after. This age-associated developmental pattern does not appear to be systematically related to whether the fiber tracts begin to myelinate early or late during brain development. That FA and DA values in earlier-myelinated tracts were greater and RD values were smaller than later-myelinated tracts does lend support to differential rates of development during prenatal, perinatal, and early childhood periods (time periods not represented in the current study). Indeed, a more recent DTI literature among healthy neonates and infants (Hermoye et al., 2006; Zhai et al., 2003) suggests that “core” white matter regions have greater FA than more peripheral regions, which ostensibly develop more rapidly during later childhood, although association fibers, such as the SLF, mature relatively late (Hermoye et al., 2006).

In terms of the degenerative trajectories examined, our hypothesis was that later-myelinated fiber tracts would show increased age-associated differences than earlier-myelinated fiber tracts. All four fiber tracts and both summary measures showed reliable differences with increasing age, but effects were greatest for the ILF (late-myelinated), CP (early-myelinated), and late-myelinated summary measures. Normal age-associated changes in ILF are similar to the report by Stricker and colleagues (Stricker et al., 2009), who showed reliable FA ILF decreases among AD patients compared with neurologically healthy age-matched controls. Consistent with our hypothesis, the finding suggests a vulnerability of later-myelinated fibers to the degeneration that occurs with normal aging and with neurodegenerative illness. This conclusion was perhaps most evident with the dissociation between early- and late-myelinated fiber summary scores, with the latter showing much more reliable age-associated differences than the former (see Figure 3, for example). However, the observation of age-related CP decline in FA and increase in RD was not consistent with our hypothesis. Further, Stricker and colleagues (Stricker et al., 2009) did not observe reliable differences between patients with AD and controls, suggesting that changes in CP may be a component of aging that is not additionally affected by neurodegenerative pathology. It is possible that certain earlier-myelinated fibers do in fact decline with normal aging and have functional significance, suggesting that the retrogenesis hypothesis does not fully capture the myriad anatomical and cognitive changes that occur with age. In a similar vein, the SLF, though an unequivocally late-myelinated tract, showed reliable but less robust age-related change, again suggesting heterogeneity in the nature of white matter decline with age.

The observation that performance on tests of executive functioning showed the largest age-associated differences is in line with several previous studies and theories of cognitive aging, which implicate executive functioning decline as a ubiquitous characteristic of normal aging (Ardila and Roselli, 1989; Drag and Bieliauskas, 2010; Gunstad et al., 2006; MacPherson et al., 2002; Rodriguez-Aranda and Sundet, 2006; Spieler et al., 1996; West, 2000; West, 1996). Because we were interested in understanding whether patterns of age-related myelin change might mediate age-associated decline in cognition, we focused on the derived executive functioning factor (i.e., the factor that showed the largest aging effect). The findings showed that FA in CP and ILF and that RD in CP mediated the relationship between age and executive functioning, suggesting that age-associated changes in white matter integrity are one source of age-related cognitive decline, but that the fiber tracts involved comprise both early- and late-myelinated systems.

We examined three components of diffusivity - - FA, RD, and DA - -, which ostensibly provide complementary information about white matter coherence and the microstructural properties of myelin. The diffusion tensor comprises three eigenvectors (represented by eigenvalues) that form an ellipsoid (Basser, 1995; Basser and Pierpaoli, 1996). Fractional anisotropy, the most common metric derived from DTI data, refers to the degree to which water is restricted in a common orientation and provides a measure of overall white matter coherence. Axial diffusivity is characterized by the largest eigenvalue in the diffusion tensor and is thought to be a measure of axonal integrity, whereas RD is the average of the second and third eigenvalue from the diffusion tensor and thought to reflect myelin integrity (Chanraud et al., 2010; Song et al., 2002; Sun et al., 2006). Thus, FA, to some extent, is a weighted summary of both RD and DA and the three metrics are not entirely independent of each other. Our data did not reveal clear dissociations between these DTI metrics, although findings tended to be most consistent for FA and RD suggesting that the observed white matter age and cognitive effects may be mediated by individual differences in myelin integrity. There were some age-related findings regarding DA; however, DA did not emerge as an important predictor of cognitive functioning in our sample, suggesting, again, that many of the observed effects with FA and RD may reflect variability in myelin integrity and axonal integrity. On the other hand, to our knowledge, the specific anatomical correlates of the different DTI metrics has been determined primarily in murine models (Song et al., 2002; Sun et al., 2006), which may not translate directly to human brains. Thus we feel that conclusions about biophysical substrates drawn from differences in DTI metrics should be considered with caution.

There have been several previous studies that have examined white matter coherence with DTI and normal cognitive aging, though they generally did not test *a priori* hypotheses about differential white matter susceptibility as a function of myelination period (Madden et al., 2009; O'Sullivan et al., 2001; Schiavone et al., 2009). Most studies have demonstrated or confirmed an anterior-to-posterior gradient of FA decline with normal aging, which appears to underlie the observed cognitive changes (Abe et al., 2002; Ardekani et al., 2007; Bucur et al., 2008; Burzynska et al., 2010; Head et al., 2004; Madden et al., 2009; Malloy et al., 2007; O'Sullivan et al., 2001; Sullivan et al., 2001; Sullivan et al., 2006; Yoon et al., 2008). Consistent with our study, those that have examined associations between DTI measures and cognition typically find that age-associated regional DTI differences are associated with age-related differences in speeded tasks of executive functioning (Madden et al., 2004; O'Sullivan et al., 2001). Salat and colleagues (Salat et al., 2005) emphasized the importance of the examination of fiber systems; unlike in our study, they found a strong reduction in FA in PLIC with age, but otherwise confirmed an anterior-to-posterior gradient of age-associated decline. Indeed, anterior regions may comprise more late-myelinated fibers than early-myelinated fibers (Pfefferbaum et al., 2000). From a systems perspective, fiber tracts that develop in support of higher order cognitive abilities (e.g., executive functioning,

language) may be more vulnerable to age-associated degeneration than fiber tracts that support more basic sensory or motor processes that develop earlier. Our data provide some, but not complete, support for this idea of “reverse recapitulation” with increasing age.

A recent study by Westlye and colleagues (Westlye et al., 2010) is one of the few other studies that has examined white matter microstructural differences in a sample comprising children, adults, and the elderly. That study also framed the hypotheses in the context of retrogenesis, but did not find clear-cut supportive evidence. Voxelwise analyses characterized early and late myelinating fibers by determining the age at peak FA values; differential rates of age-related decline were estimated by determination of the age of inflection at which time downward trajectories begin. The authors found that fibers in frontal and occipital regions as well as in parts of the forceps minor and cortical spinal tract showed relatively earlier maturation than other areas. Fibers in the SLF and cortical spinal tract showed patterns of early deterioration, whereas fibers in the dorsal cingulum bundles and uncinate showed relatively late deterioration. Thus, their findings, like ours, showed some support for a retrogenesis pattern, but also suggest that the retrogenesis hypothesis is perhaps overly simplistic to explain patterns of late-life white matter change.

There were several strengths to the present study. First, there was good representation of subjects across the lifespan. Whereas most other DTI studies of aging typically examine either the development trajectory or the degenerative trajectory, we were able to examine both in a single cohort. Second, we employed state-of-the-art DTI analysis, which was implemented systematically across subjects. Third, participants were evaluated with a standardized, well validated, comprehensive neuropsychological battery. These strengths should be interpreted in the context of some relative weaknesses. Like many studies of aging, the data we present are cross-sectional and may slightly misrepresent the true trajectories of age-associated change. Second, we were unable to scan individuals less than 7-years-old, including infants. Developmental trajectories during this time period may be critical in differential characterization of early *versus* late myelinated fibers. Third, the relatively low resolution of the DTI data likely contributed to partial volume effects and may have increased susceptibility to crossing fiber tracts, which may be differentially represented in specific fiber tracts included in the current analyses. Finally, other factors besides degree of myelination may be contributing to DTI metrics, including changes in alignment due to pathological tissue or crossing fibers (Wheeler-Kingshott and Cercignani, 2009).(Beaulieu and Allen, 1994).

In conclusion, while we did find some support for the white matter retrogenesis hypothesis in the context of normal cognitive aging, the findings were not unequivocal. Nonetheless, the examination of individual differences in white matter development and degeneration remains an important area of research given the importance of white matter in cognitive development and age-associated decline. Further, this study adds to a growing body of work that takes a *life course* perspective in understanding early-life determinants of later-life cognitive decline. To this end, future studies should examine environmental and biological factors that contribute to individual differences in white matter and their impact on cognition.

Acknowledgments

We acknowledge the data and support provided by BRAINnet; www.BRAINnet.net, under the governance of the BRAINnet Foundation. BRAINnet is the scientific network that coordinates access to the Brain Resource International Database for independent scientific purposes. We also thank the individuals who gave their time to participate in the database. This research was approved by local ethics committees. Dr. Brickman’s work is supported by NIH grants AG029949 and AG034189, and by a grant from the Alzheimer’s Association.

References

Andersson, JLR.; Jenkinson, M.; Smith, S. Non-linear optimisation. FMRIB technical report TR07JA1. 2007a. from www.fmrib.ox.ac.uk/analysis/techrep

Andersson, JLR.; Jenkinson, M.; Smith, S. Non-linear registration, aka spatial normalisation. FMRIB technical report TR07JA2. 2007b. from www.fmrib.ox.ac.uk/analysis/techrep

Ardekani S, Kumar A, Bartzokis G, Sinha U. Exploratory voxel-based analysis of diffusion indices and hemispheric asymmetry in normal aging. Magn Reson Imaging. 2007; 25:154–67. [PubMed: 17275609]

Ardila A, Roselli M. Neuropsychological characteristics of normal aging. Dev Neuropsychol. 1989; 5:307–320.

Barkovich AJ. Concepts of myelin and myelination in neuroradiology. AJNR Am J Neuroradiol. 2000; 21:1099–109. [PubMed: 10871022]

Baron RM, Kenny DA. The moderator-mediator variable distinction in social psychological research: conceptual, strategic, and statistical considerations. J Pers Soc Psychol. 1986; 51:1173–82. [PubMed: 3806354]

Bartzokis G. Alzheimer's disease as homeostatic responses to age-related myelin breakdown. Neurobiol Aging. 2009

Bartzokis G, Cummings JL, Sultzer D, Henderson VW, Nuechterlein KH, Mintz J. White matter structural integrity in healthy aging adults and patients with Alzheimer disease: a magnetic resonance imaging study. Arch Neurol. 2003; 60:393–8. [PubMed: 12633151]

Bartzokis G, Lu PH, Mintz J. Human brain myelination and amyloid beta deposition in Alzheimer's disease. Alzheimers Dement. 2007; 3:122–5. [PubMed: 18596894]

Basser PJ. Inferring microstructural features and the physiological state of tissues from diffusion-weighted images. NMR Biomed. 1995; 8:333–44. [PubMed: 8739270]

Basser PJ, Jones DK. Diffusion-tensor MRI: theory, experimental design and data analysis - a technical review. NMR Biomed. 2002; 15:456–67. [PubMed: 12489095]

Basser PJ, Pierpaoli C. Microstructural and physiological features of tissues elucidated by quantitative-diffusion-tensor MRI. J Magn Reson B. 1996; 111:209–19. [PubMed: 8661285]

Beaulieu C, Allen PS. Determinants of anisotropic water diffusion in nerves. Magn Reson Med. 1994; 31:394–400. [PubMed: 8208115]

Braak H, Braak E. Evolution of the neuropathology of Alzheimer's disease. Acta Neurol Scand Suppl. 1996; 165:3–12. [PubMed: 8740983]

Braak H, Del Tredici K, Schultz C, Braak E. Vulnerability of select neuronal types to Alzheimer's disease. Ann N Y Acad Sci. 2000; 924:53–61. [PubMed: 11193802]

Brain Resource. IntegNeuro(TM) Assessment Manual, V1.3. Brain Resource; 2010.

Brickman AM, Zahra A, Muraskin J, Steffener J, Holland CM, Habeck C, Borogovac A, Ramos MA, Brown TR, Asllani I, Stern Y. Reduction in cerebral blood flow in areas appearing as white matter hyperintensities on magnetic resonance imaging. Psychiatry Research: Neuroimaging. 2009; 15:117–120.

Brickman AM, Zimmerman ME, Paul RH, Grieve SM, Tate DF, Cohen RA, Williams LM, Clark CR, Gordon E. Regional white matter and neuropsychological functioning across the adult lifespan. Biol Psychiatry. 2006; 60:444–53. [PubMed: 16616725]

Brody BA, Kinney HC, Kloman AS, Gilles FH. Sequence of central nervous system myelination in human infancy. I. An autopsy study of myelination. J Neuropathol Exp Neurol. 1987; 46:283–301. [PubMed: 3559630]

Bucur B, Madden DJ, Spaniol J, Provenzale JM, Cabeza R, White LE, Huettel SA. Age-related slowing of memory retrieval: contributions of perceptual speed and cerebral white matter integrity. Neurobiol Aging. 2008; 29:1070–9. [PubMed: 17383774]

Burgel U, Amunts K, Hoemke L, Mohlberg H, Gilsbach JM, Zilles K. White matter fiber tracts of the human brain: three-dimensional mapping at microscopic resolution, topography and intersubject variability. Neuroimage. 2006; 29:1092–105. [PubMed: 16236527]

Chanraud S, Zahr N, Sullivan EV, Pfefferbaum A. MR diffusion tensor imaging: a window into white matter integrity of the working brain. Neuropsychol Rev. 2010; 20:209–25. [PubMed: 20422451]

Choi SJ, Lim KO, Monteiro I, Reisberg B. Diffusion tensor imaging of frontal white matter microstructure in early Alzheimer's disease: a preliminary study. J Geriatr Psychiatry Neurol. 2005; 18:12–9. [PubMed: 15681623]

Clark CR, Paul RH, Williams LM, Arns M, Fallahpour K, Handmer C, Gordon E. Standardized assessment of cognitive functioning during development and aging using an automated touchscreen battery. Arch Clin Neuropsychol. 2006; 21:449–67. [PubMed: 16904862]

Damoiseaux JS, Smith SM, Witter MP, Sanz-Arigita EJ, Barkhof F, Scheltens P, Stam CJ, Zarei M, Rombouts SA. White matter tract integrity in aging and Alzheimer's disease. Hum Brain Mapp. 2009; 30:1051–9. [PubMed: 18412132]

Drag LL, Bieliauskas LA. Contemporary review 2009: cognitive aging. J Geriatr Psychiatry Neurol. 2010; 23:75–93. [PubMed: 20101069]

Dubois J, Hertz-Pannier L, Dehaene-Lambertz G, Cointepas Y, Le Bihan D. Assessment of the early organization and maturation of infants' cerebral white matter fiber bundles: a feasibility study using quantitative diffusion tensor imaging and tractography. Neuroimage. 2006; 30:1121–32. [PubMed: 16413790]

Fellgiebel A, Schermuly I, Gerhard A, Keller I, Albrecht J, Weibrich C, Muller MJ, Stoeter P. Functional relevant loss of long association fibre tracts integrity in early Alzheimer's disease. Neuropsychologia. 2008; 46:1698–706. [PubMed: 18243252]

Gordon E, Cooper N, Rennie C, Hermens D, Williams LM. Integrative neuroscience: the role of a standardized database. Clin EEG Neurosci. 2005; 36:64–75. [PubMed: 15999901]

Grieve SM, Williams LM, Paul RH, Clark CR, Gordon E. Cognitive aging, executive function, and fractional anisotropy: a diffusion tensor MR imaging study. AJNR Am J Neuroradiol. 2007; 28:226–35. [PubMed: 17296985]

Gunstad J, Paul RH, Brickman AM, Cohen RA, Arns M, Roe D, Lawrence JJ, Gordon E. Patterns of cognitive performance in middle-aged and older adults: A cluster analytic examination. J Geriatr Psychiatry Neurol. 2006; 19:59–64. [PubMed: 16690989]

Head D, Buckner RL, Shimony JS, Williams LE, Akbudak E, Conturo TE, McAvoy M, Morris JC, Snyder AZ. Differential vulnerability of anterior white matter in nondemented aging with minimal acceleration in dementia of the Alzheimer type: evidence from diffusion tensor imaging. Cereb Cortex. 2004; 14:410–23. [PubMed: 15028645]

Hemdan S, Almazan G. Iron contributes to dopamine-induced toxicity in oligodendrocyte progenitors. Neuropathol Appl Neurobiol. 2006; 32:428–40. [PubMed: 16866988]

Hermoye L, Saint-Martin C, Cosnard G, Lee SK, Kim J, Nassogne MC, Menten R, Clapuyt P, Donohue PK, Hua K, Wakana S, Jiang H, van Zijl PC, Mori S. Pediatric diffusion tensor imaging: normal database and observation of the white matter maturation in early childhood. Neuroimage. 2006; 29:493–504. [PubMed: 16194615]

Hickie IB, Davenport TA, Naismith SL, Scott EM. SPHERE: a national depression project. SPHERE National Secretariat. Med J Aust. 2001; 175(Suppl):S4–5. [PubMed: 11556435]

Homae F, Watanabe H, Otobe T, Nakano T, Go T, Konishi Y, Taga G. Development of global cortical networks in early infancy. J Neurosci. 2010; 30:4877–82. [PubMed: 20371807]

Hua K, Zhang J, Wakana S, Jiang H, Li X, Reich DS, Calabresi PA, Pekar JJ, van Zijl PC, Mori S. Tract probability maps in stereotaxic spaces: analyses of white matter anatomy and tract-specific quantification. Neuroimage. 2008; 39:336–47. [PubMed: 17931890]

Huang H. Structure of the Fetal Brain: What We Are Learning from Diffusion Tensor Imaging. Neuroscientist. 2010; 16:634–639. [PubMed: 20360600]

Huang H, Xue R, Zhang J, Ren T, Richards LJ, Yarowsky P, Miller MI, Mori S. Anatomical characterization of human fetal brain development with diffusion tensor magnetic resonance imaging. J Neurosci. 2009; 29:4263–73. [PubMed: 19339620]

Huang H, Zhang J, Wakana S, Zhang W, Ren T, Richards LJ, Yarowsky P, Donohue P, Graham E, van Zijl PC, Mori S. White and gray matter development in human fetal, newborn and pediatric brains. Neuroimage. 2006; 33:27–38. [PubMed: 16905335]

Huppi PS. Growth and development of the brain and impact on cognitive outcomes. Nestle Nutr Workshop Ser Pediatr Program. 2010; 65:137–49. discussion 149–51.

Huppi PS, Maier SE, Peled S, Zientara GP, Barnes PD, Jolesz FA, Volpe JJ. Microstructural development of human newborn cerebral white matter assessed in vivo by diffusion tensor magnetic resonance imaging. Pediatr Res. 1998; 44:584–90. [PubMed: 9773850]

Huttenlocher PR, Dabholkar AS. Regional differences in synaptogenesis in human cerebral cortex. J Comp Neurol. 1997; 387:167–78. [PubMed: 9336221]

Kinney HC, Brody BA, Kloman AS, Gilles FH. Sequence of central nervous system myelination in human infancy. II. Patterns of myelination in autopsied infants. J Neuropathol Exp Neurol. 1988; 47:217–34. [PubMed: 3367155]

Kochunov P, Williamson DE, Lancaster J, Fox P, Cornell J, Blangero J, Glahn DC. Fractional anisotropy of water diffusion in cerebral white matter across the lifespan. Neurobiol Aging. 2010

Le Bihan D, Mangin JF, Poupon C, Clark CA, Pappata S, Molko N, Chabriat H. Diffusion tensor imaging: concepts and applications. J Magn Reson Imaging. 2001; 13:534–46. [PubMed: 11276097]

MacPherson SE, Phillips LH, Della Sala S. Age, executive function, and social decision making: a dorsolateral prefrontal theory of cognitive aging. Psychol Aging. 2002; 17:598–609. [PubMed: 12507357]

Madden DJ, Spaniol J, Costello MC, Bucur B, White LE, Cabeza R, Davis SW, Dennis NA, Provenzale JM, Huettel SA. Cerebral white matter integrity mediates adult age differences in cognitive performance. J Cogn Neurosci. 2009; 21:289–302. [PubMed: 18564054]

Madden DJ, Whiting WL, Huettel SA, White LE, MacFall JR, Provenzale JM. Diffusion tensor imaging of adult age differences in cerebral white matter: relation to response time. Neuroimage. 2004; 21:1174–81. [PubMed: 15006684]

Makris N, Papadimitriou GM, van der Kouwe A, Kennedy DN, Hodge SM, Dale AM, Benner T, Wald LL, Wu O, Tuch DS, Caviness VS, Moore TL, Killiany RJ, Moss MB, Rosene DL. Frontal connections and cognitive changes in normal aging rhesus monkeys: a DTI study. Neurobiol Aging. 2007; 28:1556–67. [PubMed: 16962214]

McLaughlin NC, Paul RH, Grieve SM, Williams LM, Laidlaw D, DiCarlo M, Clark CR, Whelihan W, Cohen RA, Whitford TJ, Gordon E. Diffusion tensor imaging of the corpus callosum: a cross-sectional study across the lifespan. Int J Dev Neurosci. 2007; 25:215–21. [PubMed: 17524591]

Milner B. Visually-guided maze learning in man: Effects of bilateral hippocampal, bilateral frontal, and unilateral cerebral lesions. Neuropsychologia. 1965; 3:317–338.

Mori S, Oishi K, Jiang H, Jiang L, Li X, Akhter K, Hua K, Faria AV, Mahmood A, Woods R, Toga AW, Pike GB, Neto PR, Evans A, Zhang J, Huang H, Miller MI, van Zijl P, Mazziotta J. Stereotaxic white matter atlas based on diffusion tensor imaging in an ICBM template. Neuroimage. 2008; 40:570–82. [PubMed: 18255316]

O'Sullivan M, Jones DK, Summers PE, Morris RG, Williams SC, Markus HS. Evidence for cortical "disconnection" as a mechanism of age-related cognitive decline. Neurology. 2001; 57:632–8. [PubMed: 11524471]

Paul RH, Lawrence J, Williams LM, Richard CC, Cooper N, Gordon E. Preliminary validity of "integneuro": a new computerized battery of neurocognitive tests. Int J Neurosci. 2005; 115:1549–67. [PubMed: 16223701]

Pfefferbaum A, Sullivan EV, Hedehus M, Lim KO, Adalsteinsson E, Moseley M. Age-related decline in brain white matter anisotropy measured with spatially corrected echo-planar diffusion tensor imaging. Magn Reson Med. 2000; 44:259–68. [PubMed: 10918325]

Pierpaoli C, Basser PJ. Toward a quantitative assessment of diffusion anisotropy. Magn Reson Med. 1996; 36:893–906. [PubMed: 8946355]

Rakic P, Bourgeois JP, Eckenhoff MF, Zecevic N, Goldman-Rakic PS. Concurrent overproduction of synapses in diverse regions of the primate cerebral cortex. Science. 1986; 232:232–5. [PubMed: 3952506]

Reisberg B, Franssen EH, Hasan SM, Monteiro I, Boksay I, Souren LE, Kenowsky S, Auer SR, Elahi S, Kluger A. Retrogenesis: clinical, physiologic, and pathologic mechanisms in brain aging, Alzheimer's and other dementing processes. Eur Arch Psychiatry Clin Neurosci. 1999; 249(Suppl 3):28–36. [PubMed: 10654097]

Reitan RM. Validity of the trail making test as an indication of organic brain damage. Perceptual and Motor Skills. 1958; 8:271–276.

Rodriguez-Aranda C, Sundet K. The frontal hypothesis of cognitive aging: factor structure and age effects on four frontal tests among healthy individuals. J Genet Psychol. 2006; 167:269–87. [PubMed: 17278416]

Salat DH, Tuch DS, Greve DN, van der Kouwe AJ, Hevelone ND, Zaleta AK, Rosen BR, Fischl B, Corkin S, Rosas HD, Dale AM. Age-related alterations in white matter microstructure measured by diffusion tensor imaging. Neurobiol Aging. 2005; 26:1215–27. [PubMed: 15917106]

Schiavone F, Charlton RA, Barrick TR, Morris RG, Markus HS. Imaging age-related cognitive decline: A comparison of diffusion tensor and magnetization transfer MRI. J Magn Reson Imaging. 2009; 29:23–30. [PubMed: 19097099]

Smith SM, Jenkinson M, Johansen-Berg H, Rueckert D, Nichols TE, Mackay CE, Watkins KE, Ciccarelli O, Cader MZ, Matthews PM, Behrens TE. Tract-based spatial statistics: voxelwise analysis of multi-subject diffusion data. Neuroimage. 2006; 31:1487–505. [PubMed: 16624579]

Smith SM, Jenkinson M, Woolrich MW, Beckmann CF, Behrens TE, Johansen-Berg H, Bannister PR, De Luca M, Drobnjak I, Flitney DE, Niazy RK, Saunders J, Vickers J, Zhang Y, De Stefano N, Brady JM, Matthews PM. Advances in functional and structural MR image analysis and implementation as FSL. Neuroimage. 2004; 23(Suppl 1):S208–19. [PubMed: 15501092]

Sobel, ME. Asymptotic intervals for indirect effects in structural equation models. In: Leinhart, S., editor. Sociological methodology. Jossey-Bass; San Francisco: 1982. p. 290-312.

Song SK, Sun SW, Ju WK, Lin SJ, Cross AH, Neufeld AH. Diffusion tensor imaging detects and differentiates axon and myelin degeneration in mouse optic nerve after retinal ischemia. Neuroimage. 2003; 20:1714–22. [PubMed: 14642481]

Song SK, Sun SW, Ramsbottom MJ, Chang C, Russell J, Cross AH. Dysmyelination revealed through MRI as increased radial (but unchanged axial) diffusion of water. Neuroimage. 2002; 17:1429–36. [PubMed: 12414282]

Song SK, Yoshino J, Le TQ, Lin SJ, Sun SW, Cross AH, Armstrong RC. Demyelination increases radial diffusivity in corpus callosum of mouse brain. Neuroimage. 2005; 26:132–40. [PubMed: 15862213]

Spieler DH, Balota DA, Faust ME. Stroop performance in healthy younger and older adults and in individuals with dementia of the Alzheimer's type. J Exp Psychol Hum Percept Perform. 1996; 22:461–79. [PubMed: 8934854]

Stricker NH, Schweinsburg BC, Delano-Wood L, Wierenga CE, Bangen KJ, Haaland KY, Frank LR, Salmon DP, Bondi MW. Decreased white matter integrity in late-myelinating fiber pathways in Alzheimer's disease supports retrogenesis. Neuroimage. 2009; 45:10–6. [PubMed: 19100839]

Sullivan EV, Adalsteinsson E, Pfefferbaum A. Selective age-related degradation of anterior callosal fiber bundles quantified in vivo with fiber tracking. Cereb Cortex. 2006; 16:1030–9. [PubMed: 16207932]

Sullivan EV, Pfefferbaum A. Diffusion tensor imaging and aging. Neurosci Biobehav Rev. 2006; 30:749–61. [PubMed: 16887187]

Sullivan EV, Rohlfing T, Pfefferbaum A. Quantitative fiber tracking of lateral and interhemispheric white matter systems in normal aging: relations to timed performance. Neurobiol Aging. 31:464–81. [PubMed: 18495300]

Sun SW, Liang HF, Le TQ, Armstrong RC, Cross AH, Song SK. Differential sensitivity of in vivo and ex vivo diffusion tensor imaging to evolving optic nerve injury in mice with retinal ischemia. Neuroimage. 2006; 32:1195–204. [PubMed: 16797189]

Sun SW, Liang HF, Schmidt RE, Cross AH, Song SK. Selective vulnerability of cerebral white matter in a murine model of multiple sclerosis detected using diffusion tensor imaging. Neurobiol Dis. 2007; 28:30–8. [PubMed: 17683944]

Takeda K, Nomura Y, Sakuma H, Tagami T, Okuda Y, Nakagawa T. MR assessment of normal brain development in neonates and infants: comparative study of T1- and diffusion-weighted images. J Comput Assist Tomogr. 1997; 21:1–7. [PubMed: 9022760]

Walsh K. Understanding Brain Damage. Churchill Livingstone, Edinburgh. 1985

Wechsler D. Wechsler Memory Scale - Three. Psychological Corporation, San Antonio. 1999

West R. In defense of the frontal lobe hypothesis of cognitive aging. J Int Neuropsychol Soc. 2000; 6:727–9. discussion 730. [PubMed: 11011518]

West RL. An application of prefrontal cortex function theory to cognitive aging. Psychol Bull. 1996; 120:272–92. [PubMed: 8831298]

Westlye LT, Walhovd KB, Dale AM, Bjornerud A, Due-Tonnessen P, Engvig A, Grydeland H, Tamnes CK, Ostby Y, Fjell AM. Life-span changes of the human brain White matter: diffusion tensor imaging (DTI) and volumetry. Cereb Cortex. 2010; 20:2055–68. [PubMed: 20032062]

Wheeler-Kingshott CA, Cercignani M. About “axial” and “radial” diffusivities. Magn Reson Med. 2009; 61:1255–60. [PubMed: 19253405]

Williams LM, Hermens DF, Thein T, Clark CR, Cooper NJ, Clarke SD, Lamb C, Gordon E, Kohn MR. Using brain-based cognitive measures to support clinical decisions in ADHD. Pediatr Neurol. 2010; 42:118–26. [PubMed: 20117748]

Williams LM, Simms E, Clark CR, Paul RH, Rowe D, Gordon E. The test-retest reliability of a standardized neurocognitive and neurophysiological test battery: “neuromarker”. Int J Neurosci. 2005; 115:1605–30. [PubMed: 16287629]

Yakovlev, PI.; Lecours, AR. Regional development of the brain in early life. In: Minkowski, A., editor. The myelogenetic cycles of regional maturation of the brain. Blackwell Scientific Publications; Boston: 1967. p. 3-65.

Zhai G, Lin W, Wilber KP, Gerig G, Gilmore JH. Comparisons of regional white matter diffusion in healthy neonates and adults performed with a 3.0-T head-only MR imaging unit. Radiology. 2003; 229:673–81. [PubMed: 14657305]

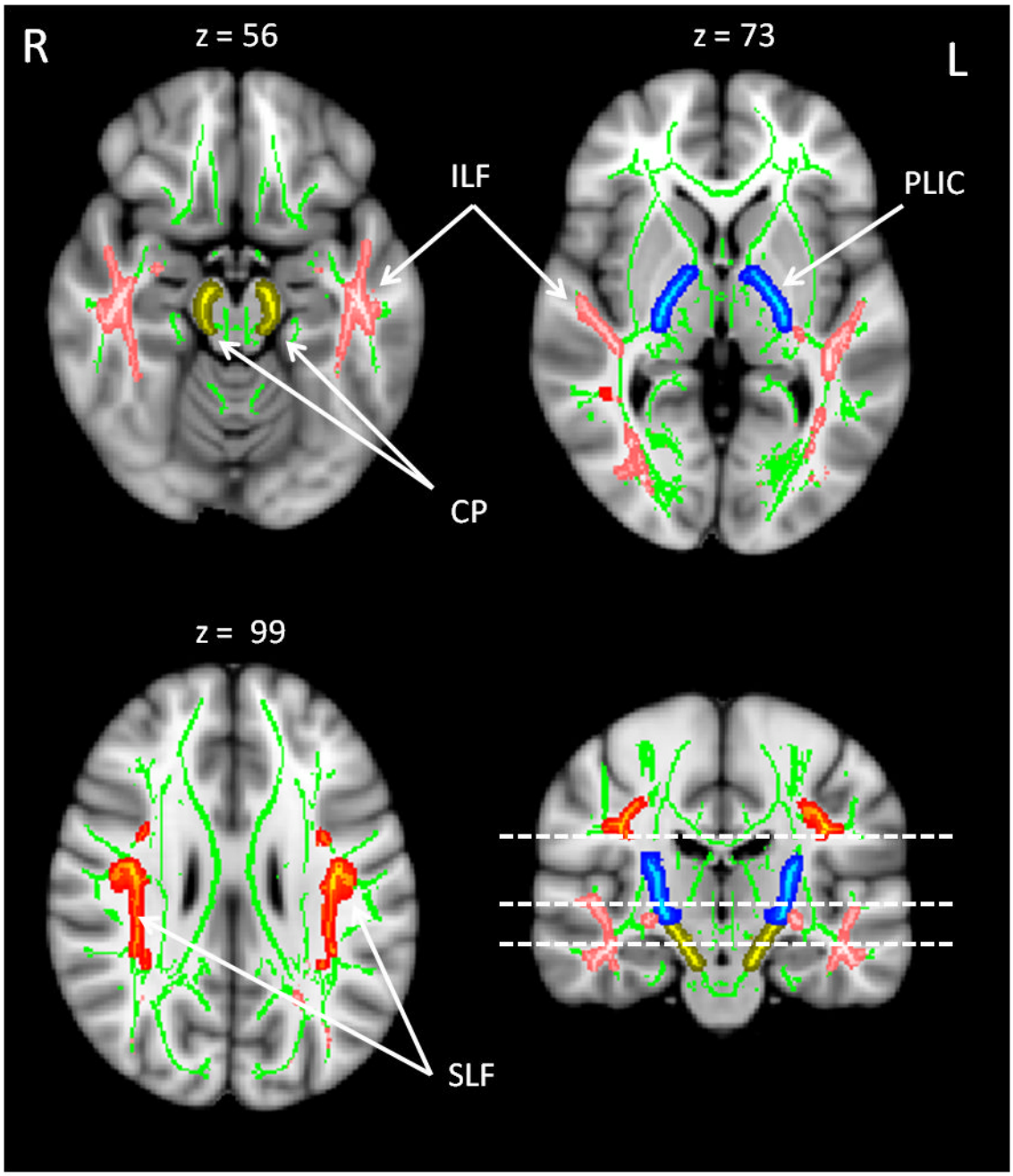

Figure 1.
Fractional anisotropy skeleton (in green) representing the major WM tracts for all subjects is overlayed on the MNI standard brain. Sections of the tract skeleton representing the prototypical early- and late-myelinated fiber bundles used in the study are marked: early posterior limb of the internal capsule (PLIC) in blue and cerebral peduncles (CP) in yellow; late superior longitudinal fasciculus (SLF) in red and inferior longitudinal fasciculus (ILF) in pink. Images are in radiological orientation R- right, L- Left.

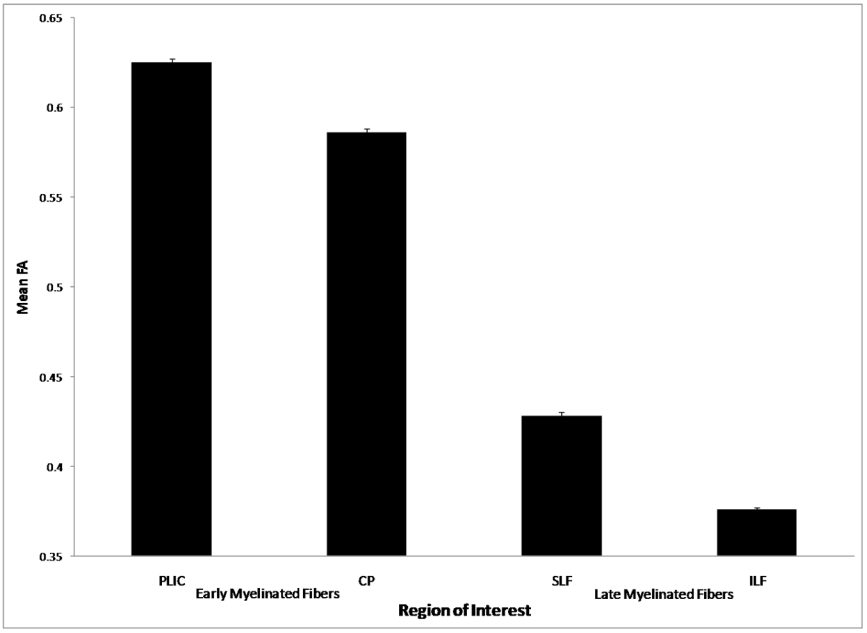

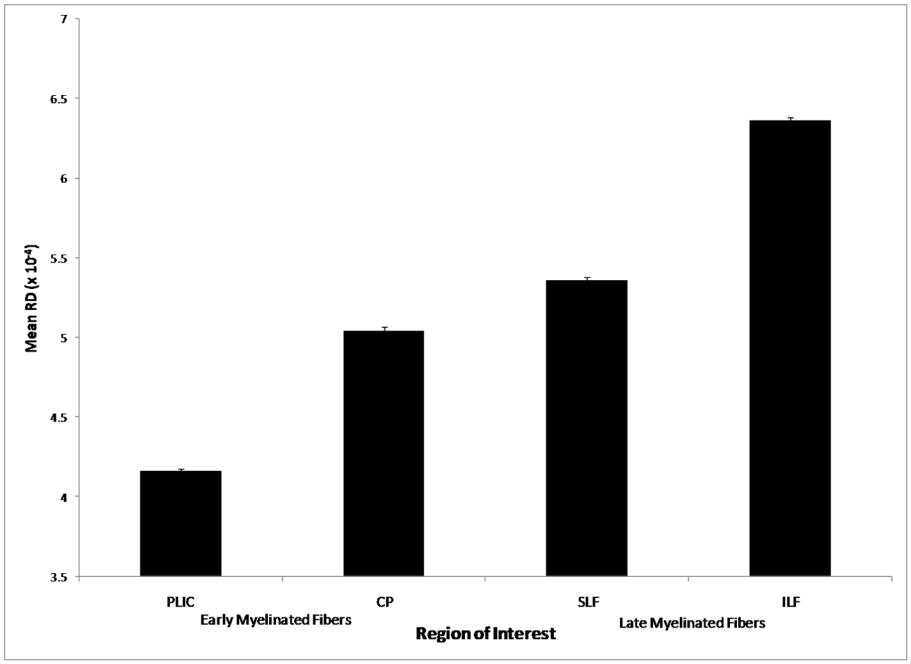

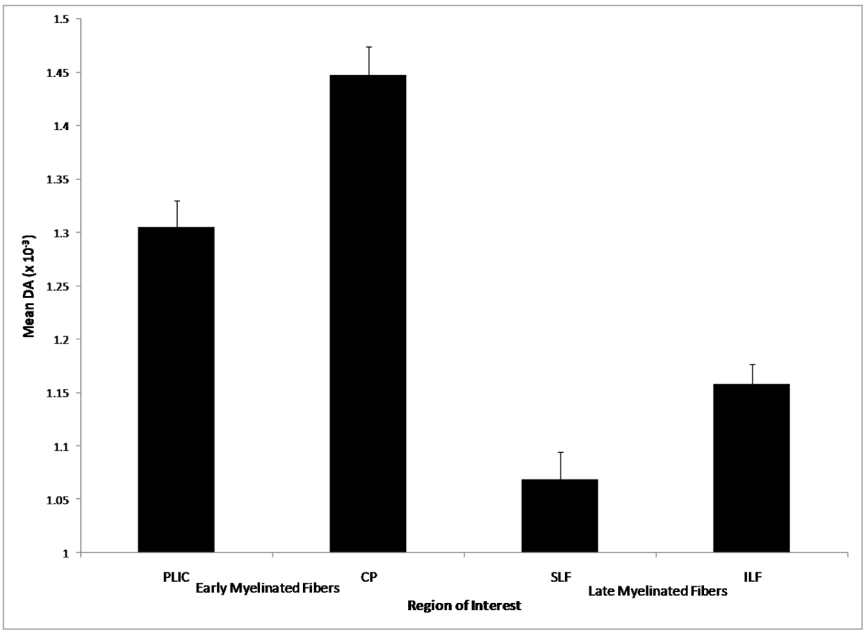

Figure 2.

Mean FA, RD, and DA (upper, middle, and lower panels, respectively) values across four regions-of-interest in the entire cohort. Values are means adjusted for age and sex. Error bars are standard errors. All pairwise comparisons (for all three metrics) are significant ($p<0.001$).

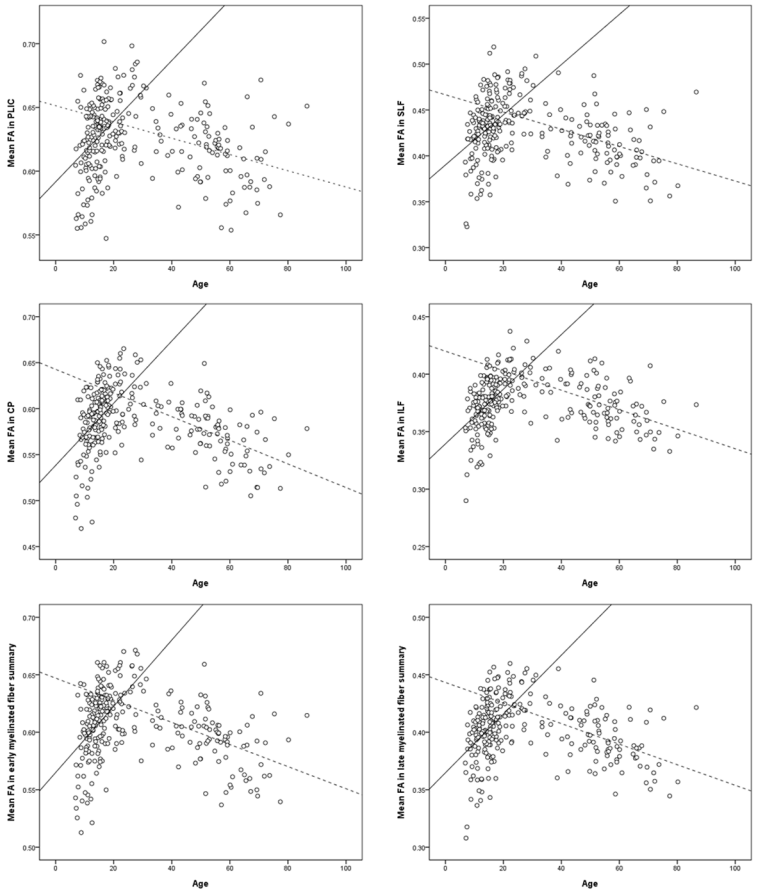

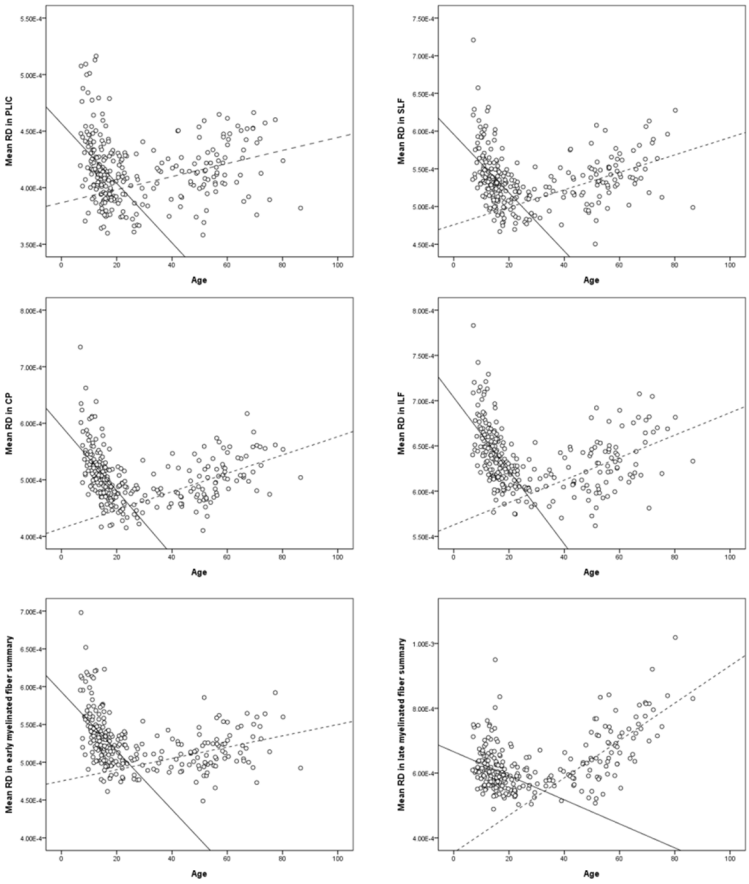

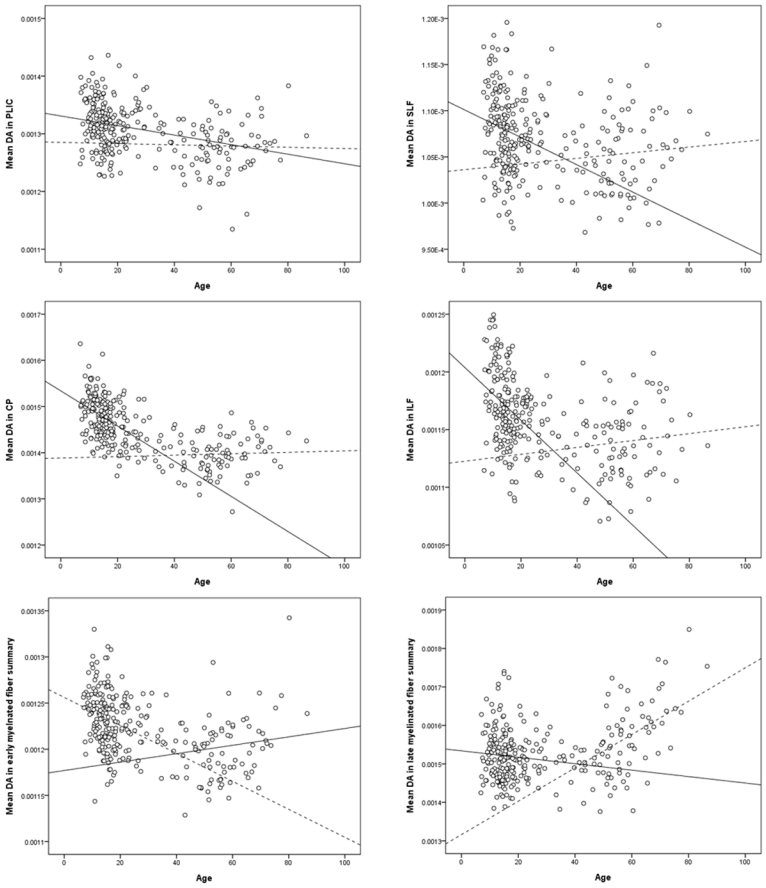

Figure 3.

Scatterplots of association between age and mean in early- (left column) and late-myelinated (right column) fiber tracts. The top 6 plots are for FA; the middle 6 plots are for RD; and the bottom 6 plots are for DA. Separate linear trend lines are superimposed for age-associated differences in the Younger Group (solid black line) and the Older Group (dotted line).

Table 1

Demographic characteristics of the two age groups and total sample.

Variable		Younger Group (7–30 years)	Older Group (31–87 years)	Total Sample
N		191	91	282
Age	Mean (SD)	15.76 (5.13)	54.16 (11.90)	28.15 (19.66)
	Range	6.85–29.46	30.25–86.55	6.85–86.55
Education	Mean (SD)	9.71 (3.99)	12.97 (3.09)	10.74 (4.02)
	Range	2–18	7–18	2–18
% female sex		46.1	44.0	45.4

Table 2

Results from the primary regression analyses comparing age with FA, RD, and DA in early- and late-myelinated fiber tracts in the two age groups. β weights are reported as standardized coefficients (β_{stand}) and raw coefficients with 95% confidence intervals (CI) indicated. Note that raw β and CI are reported as 10^{-3} for FA, as 10^{-6} for RD and DA. All models control for sex (where 0=male, 1=female). For FA, sex only entered significantly into the SLF (β_{stand} =−0.309, p=0.001) and early fiber summary (β_{stand} =−0.255, p=0.012) models in the Older Group. For RD, sex entered significantly into the model for the late fiber summary score among older adults only (β_{stand}=−0.205, p=0.003). For DA, sex entered significantly into all models except for CP among older adults, ILF among younger adults, and early fiber summary (all β_{stand}'s>-0.149, all p's<0.04).

			Younger Group (7–30 years)			Older Group (31–87 years)		
			Overall model (df=2,190)	**Age β_{stand}**	**Age β (CI)**	**Overall model (df=2,90)**	**Age β**	**Age β (CI)**
FA	Early fibers	PLIC	F=20.14***	0.418***	2.39(1.64, 3.15)	F=5.25*	−0.289**	−0.639 (−0.12, −0.20)
		CP	F=30.40***	0.492***	3.40(2.54,4.27)	F=16.84***	−0.521***	−1.29(−1.73,−8.42)
		Early fiber summary	F=25.95***	0.465***	2.84(2.06,3.61)	F=7.16***	−0.275*	−0.54(−0.92,−0.15)
	Late fibers	SLF	F=21.87***	0.429***	2.75(1.91,3.58)	F=13.02***	−0.366***	−0.94(−0.14,−0.46)
		ILF	F=38.25***	0.536***	2.37(1.84,2.91)	F=14.56***	−0.486***	−0.85(−−1.17,−0.53)
		Late fiber summary	F=19.75***	0.393***	2.54(1.70,3.39)	F=31.55***	−0.645***	−2.05(−2.56,−1.54)
RD	Early fibers	PLIC	F=22.60***	−0.441***	−2.46(−3.41,−1.86)	F=3.72***	0.279***	0.57(0.16,1.00)
		CP	F=54.26***	−0.605***	−5.70(−6.79,−4.62)	F=15.04***	0.504***	1.59(0.64,1.68)
		Early fiber summary	F=40.63***	−0.547***	−3.88(−4.74,−3.03)	F=5.917**	0.341***	0.75(0.31,0.12)
	Late fibers	SLF	F=39.42***	−0.540***	−3.86(−4.72,−3.00)	F=9.89***	0.428***	1.16(0.64,0.17)
		ILF	F=59.95***	−0.612***	−4.02(−4.76,−3.28)	F=13.64***	0.471***	1.24(0.75,1.73)
		Late fiber summary	F=14.75***	−0.297***	−3.59(−5.22,−1.97)	F=50.633***	0.699***	5.76(4.57,6.96)
DA	Early fibers	PLIC	F=3.20*	−0.097	−0.77(−1.90,0.53)	F=2.99	−0.029	−0.11(−0.88,0.66)
		CP	F=24.21***	−0.407***	−3.73(−4.91,−2.55)	F=0.363	0.046	0.15(−0.55,8.61)
		Early fiber summary	F=7.17***	−0.244***	−1.49(−2.34,−0.64)	F=6.41**	0.157	0.45(−0.12,1.02)
	Late fibers	SLF	F=5.83**	−0.172*	−1.43(−2.59,−0.27)	F=12.63***	0.081	0.30(−0.39,−0.99)
		ILF	F=15.48***	−0.348***	−2.25(−3.11,−1.39)	F=7.06***	0.111	2.96(−2.28,8.19)
		Late fiber summary	F=4.72*	−0.056	−0.72(−2.51,−0.11)	F=40.933***	0.552***	4.32(3.13,5.52)

*** p≤0.001,

** p≤.005,

* p≤0.05

Table 3

Factor loadings for neuropsychological test scores derived in the Older Group. Only loadings >0.50 are displayed.

Variable	Factor			
	1	2	3	4
Verbal Memory total learning score		0.989		
Verbal Memory short delay free recall		0.919		
Verbal Memory long delay free recall		0.958		
Word Generation: letter fluency (FAS)				0.828
Word Generation: category fluency (Animal naming)				0.711
Motor Tapping (dominant hand)			0.829	
Choice Reaction Time	−0.715			
Span of Visual Memory (recall span)	0.720			
Digit Span forward			0.722	
Digit Span backward			0.817	
Switching of Attention 1	−0.829			
Switching of Attention 2	−0.773			
Mazes task	−0.769			

Table 4

Results from regression analyses examining association of mean FA, RD, and DA values within early- and late-myelinated fiber tracts with executive functioning within the Older Group. Standardized regression coefficients are displayed for the primary variable of interests (i.e., age, mean FA) and covariates in the model (i.e., education, sex).

		Early myelinated fiber tracts			Late myelinated fiber tracts		
		PLIC	**CP**	**Early fiber summary**	**SLF**	**ILF**	**Late fiber summary**
FA	Overall model (df=4,26)	F=6.175 **	F=8.751 ***	F=5.22 **	F=6.206 **	F=7.969 ***	F=6.07 **
	Age β	−0.683 ***	−0.573 ***	−0.670 ***	−0.672 ***	−0.593 ***	−0.554 *
	Education β	−0.376 *	−0.489 **	−0.394 *	−0.383 *	−0.380 *	−0.370 *
	Sex β	−0.184	−0.271	−0.155	−0.134	−0.111	−0.919
	Mean FA within tract β	0.244	0.435 *	0.138	0.250	0.366 *	0.271
RD	Overall model (df=4,26)	F=0.633	F=7.424 ***	F=5.699 **	F=6.168 **	F=6.283 **	F=5.622 **
	Age β	−0.721 ***	−0.604 ***	−0.675 ***	−0.657 ***	−0.644 ***	−0.502 *
	Education β	−0.424 *	−0.437 *	−0.438 *	−0.425 *	−0.437 *	−0.391 *
	Sex β	−0.229	−0.262	−0.185	−0.194	−0.228	−0.211
	Mean RD within tract β	−0.246	−0.360 *	−0.211	−0.254	−0.273	−0.283
DA	Overall model (df=4,26)	F=4.874 *	F=4.874 *	F=5.302 *	F=4.895 *	F=4.870 *	F=4.880 *
	Age β	−0.691 ***	−0.695 ***	−0.718 ***	−0.691 ***	−0.695 ***	−0.674 *
	Education β	−0.365 *	−0.368 *	−0.4.34 *	−0.382 *	−0.371 *	−0.374 *
	Sex β	−0.171	−0.175	−0.237	−0.190	−0.175	−0.186
	Mean DA within tract β	0.015	−0.094	−0.164	−0.041	−0.003	−0.036

*** p≤0.001,

** p≤.005,

* p≤0.05